

Research Article



Protective Effect of A New Peptide HS1002 Against Cisplatin-Induced Acute **Kidney Injury**

Joo Hee Han, Hyun Ji Noh, Ju Ri Kim, Haeun Lee, Jae Hyeon Park, Hyung Sik Kim*

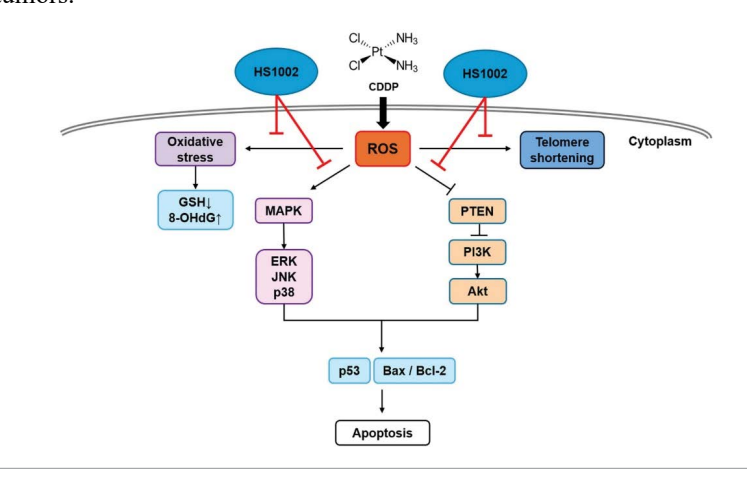
Abstract

Background: The administration of the chemotherapeutic agent cisplatin (CDDP) to patients with cancer is limited by the occurrence of acute kidney injury (AKI), with no effective protective therapies currently available. The present study investigated the protective effects of HS1002 against CDDP-induced nephrotoxicity in Sprague-Dawley rats.

Methods: HS 1002 was administered subcutaneously at 10 mg/kg for 3 days consecutively, following intraperitoneal injection of CDDP (6 mg/kg). All rats were euthanized 72 h after CDDP administration. Histopathological examination, AKI biomarkers, apoptosis, and oxidative damage were evaluated.

Results: HS1002 protected against CDDP-induced cytotoxicity and apoptotic cell death in rats. The CDDP-induced elevation of serum blood urea nitrogen (BUN) and creatinine (sCr) levels were significantly ameliorated by HS1002. Additionally, urinary excretion of kidney injury markers, including kidney injury molecule-1 (KIM-1), selenium-binding protein-1 (SBP-1), and neutrophil gelatinase-associated lipocalin (NGAL), were significantly reduced. Furthermore, HS1002 markedly improved antioxidant enzyme activities and reduced DNA damage in CDDP-treated rat kidneys. Notably, HS1002 administration inhibited telomere shortening and restored apoptosis regulation through the extracellular signal-regulated kinase signaling pathway, enhancing protection against renal injury. Histopathological examinations confirmed the HS1002 protective effects against CDDP-induced renal injury. However, HS1002 did not affect the anticancer activity of CDDP in the tumor xenograft model.

Conclusions: These findings suggest that HS1002 is a potential adjuvant therapy in cancer patients with undergoing CDDP therapy by preventing CDDP-induced nephrotoxicity. Collectively, HS1002 may serve as a therapeutic agent for preventing CDDP-induced AKI in patients with solid tumors.



Affiliation:

Lab. of Molecular Toxicology, School of Pharmacy, Sungkyunkwan University, Seobu-ro, 2066, Jangan-gu, Suwon 16419, Republic of Korea

*Corresponding author:

Hyung Sik Kim, Lab. of Molecular Toxicology, School of Pharmacy, Sungkyunkwan University, Seobu-ro, 2066, Jangan-gu, Suwon 16419, Republic of Korea.

Citation: Joo Hee Han, Hyun Ji Noh, Ju Ri Kim, Haeun Lee, Jae Hyeon Park, Hyung Sik Kim. Protective Effect of A New Peptide HS1002 Against Cisplatin-Induced Acute Kidney Injury. Journal of Biotechnology and Biomedicine. 8 (2025): 331-344.

Received: April 16, 2025 Accepted: April 30, 2025 Published: November 04, 2025



Keywords: Cisplatin; HS1002; Nephrotoxicity; Urinary biomarker; Chemosensitivity

Introduction

Cisplatin (CDDP) is one of the most effective chemotherapeutic agents widely used to treat malignant neoplasms affecting various organs, including the stomach, ovaries, cervix, head, neck, testicles, and bladder [1,2]. However, the therapeutic utility of CDDP is limited due to the occurrence of severe toxicities such as neurotoxicity, ototoxicity, nausea, vomiting, and nephrotoxicity in patients with cancer. Among these, nephrotoxicity is the most common and severe [3,4]. Numerous studies have shown that several processes such as the accumulation and metabolic activation of harmful substances in the kidneys, DNA damage, and apoptosis are intricately associated with CDDP-induced nephrotoxicity [5-9]. The most significant renal damage caused by CDDP is characterized by severe proximal tubular cell death involving both necrosis and apoptosis [4,8,10]. However, the precise molecular mechanisms underlying CDDP-induced acute kidney injury (AKI) remain unclear.

Multiple lines of evidence have demonstrated that reactive oxygen species (ROS) production and the resulting oxidative stress play significant roles in the pathogenesis of AKI induced by CDDP [11-14]. Excessive ROS production can cause oxidative damage to DNA and proteins as well as lipid peroxidation, leading to various forms of cellular damage. Overexposure to ROS also triggers programmed cell death (apoptosis), which is strongly associated with CDDP-induced kidney failure [15]. In addition, CDDP stimulates the activation of mitogen-activated protein kinase (MAPK) pathways. Specifically, the activation of apoptotic caspases, inflammation, and kidney damage can be inhibited by pharmacological or genetic inhibitors targeting c-Jun N-terminal kinase (JNK), extracellular signal-regulated kinases 1 and 2 (ERK1/2), and p38 MAPK [16]. Numerous studies have focused on elucidating the mechanisms underlying CDDP-induced nephrotoxicity; however, no successful treatment is currently available to prevent CDDPinduced AKI. Therefore, it is crucial to develop more effective preventive strategies to mitigate CDDP-induced AKI in patients with cancer.

Recently, peptides have gained prominence as a novel class of therapeutic drugs owing to their distinctive biochemical properties and potential therapeutic applications [17]. Food and Drug Administration (FDA)-approved drugs are typically classified into three major groups: small-molecule drugs, biologics, and peptides. Among these, peptides drugs constitute approximately 6% of the total [18]. Over 100 peptide drugs have been approved owing to the growing demand for peptide therapeutics. Unlike small-molecule drugs, peptide drugs offer several advantages

including enhanced specificity, effectiveness, and stability [19]. Moreover, compared to biologics, peptide drugs possess distinct benefits such as reduced immunogenicity and improved membrane permeability. These attributes contribute to their notable clinical efficacy and absence of metabolic toxicity, making them a focus of extensive global research and development efforts [20]. Peptides can be modified in a site-specific manner through chemical synthesis or genetic code expansion, to further improve their stability and physiological activity [21,22].

A previous study demonstrated that certain peptide drugs exhibit a protective effect against kidney injury by reducing apoptosis in kidney tissues [23]. Furthermore, gonadotropinreleasing hormone (GnRH) receptors are present in kidney tissue, and leuprolide acetate, a GnRH agonist, protects against CDDP-induced kidney damage [24]. Recent studies have shown that the 9-amino acid sequence of the hTERT:611-626 peptide (Ile-Phe-Arg-Leu-Arg-Ser-Thr-Leu-Leu) is similar to that of several other GnRH analogs. This sequence includes a Leu-Arg region that plays a critical role in determining ligand selectivity [7,23]. Based on these findings, unique peptides were developed through amino acid modifications and alterations to the Leu-Arg region of hTERT:611-626 peptide. A new peptide drug, HS1002 (pGlu-His-Trp-Ser-Tyr-Arg-Leu-Arg-Phe-Ile-Pro-NHEt), which is based on the structures of GnRH and hTERT, potentially has a protective effect against nephrotoxicity. This study aimed to investigate the protective effects of HS1002 against CDDPinduced nephrotoxicity in vivo and elucidate the molecular mechanisms underlying the protective activity of HS1002 in CDDP-induced AKI.

Materials and Methods

Chemicals

Peptides were synthesized using the solid-phase peptide synthesis technique described by Anygen (Gwangju, Korea). Peptide solution was prepared in Dulbecco's phosphate-buffered saline (DPBS). The primary antibodies were purchased from Abcam (Cambridge, USA). Horseradish peroxidase (HRP)-conjugated secondary antibody was purchased from Santa Cruz Biotechnology (Santa Cruz, CA, USA). All other reagents were purchased from Sigma-Aldrich (St. Louis, MO, USA).

Experimental design

Male Sprague–Dawley (SD) rats (6 weeks old, 200 \pm 5 g) were obtained from Charles River Laboratory Animal Resources (OrientBio, Sungnam, Korea). All animals were housed in a controlled environment in a specific pathogen-free (SPF) room, with lighting set to a 12-h light/dark cycle. The ambient temperature was maintained between 21–25 °C, and the relative humidity was kept at 55%. The rats had



ad libitum access to tap water and food. The experimental protocol was approved by the Institutional Animal Care and Use Committee of Sungkyunkwan University (SKKUIACUC2023-09-20-1). CDDP was dissolved in DPBS and administered intraperitoneally (i.p.) to rats as a single dose to induce nephrotoxicity. Rats were divided into four groups (n = 6 per group; Figure 1). The groups were as follows: vehicle control (DPBS, i.p.), CDDP (6 mg/kg, i.p.), HS1002 (10 mg/kg, s.c.), and CDDP + HS1002 pretreatment (10 mg/kg, s.c., once daily for 3 days prior to a single CDDP injection). At the end of the experiment, all animals were euthanized after fasting for 24 h. Kidneys were isolated for histological and other analyses. Blood samples were collected 60 min post-administration, and serum was separated through centrifugation at 1500 × g. Kidney and serum samples were immediately stored at -80 °C until further analysis.

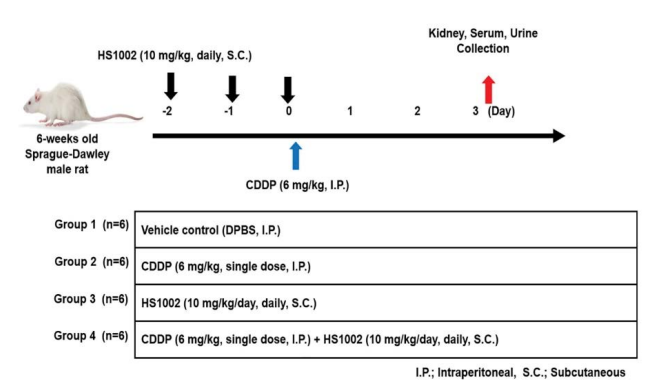


Figure 1: Experimental design to cisplatin (CDDP)-induce nephrotoxicity in rats. Rats were randomly divided into four groups: control (DPBS), HS1002 (10 mg/(kg·d), subcutaneous [s.c.] injection, CDDP (6 mg/kg, single intraperitoneal [i.p.] injection), and CDDP (6 mg/kg, single i.p. injection) + HS1002 (10 mg/kg/d) groups. HS1002 was injected for 3 days.

Urinalysis and serum biochemical analysis

For urine collection, the animals were placed in metabolic cages for 24 h before euthanasia. Total urine samples were collected over a 24 h period, and the exact volume of urine was recorded. The samples were immediately centrifuged at 900 × g for 10 min to remove any impurities. Urine samples stored at -80 °C were slowly thawed at 4 °C for analysis. The rats underwent overnight fasting and were anesthetized using CO₂ exposure. Blood was collected from the abdominal aorta and immediately centrifuged at 1500 × g for 10 min. The resulting serum samples were promptly stored at -80 °C until analysis. Biochemical analyses of various parameters, including serum creatinine (sCr) and blood urea nitrogen (BUN), were performed using a Hitachi 912 Automatic Analyzer (Roche Diagnostics, Sandhofer, Mannheim, Germany).

Biochemical analysis

The activities of BUN, sCr, aspartate transaminase, and alanine transaminase were measured using a Hitachi 912 Automatic Analyzer (Roche Diagnostics, Mannheim, Germany). After the animals were anesthetized, their kidneys were promptly frozen in liquid nitrogen and weighed.

Histopathological examination

After sacrificing the rats, their kidneys were excised and fixed in 10% neutral buffered formalin for a minimum of 24 h. The tissue from the right kidney was embedded in paraffin and sliced into 5 µm thick sections. Several consecutive paraffin sections were deparaffinized using xylene (three times for 5 minutes each), hydrated in a graded alcohol series, rinsed with deionized water, and stained with hematoxylin and eosin for 1 min. Renal injury scores were assessed by three independent researchers in a blinded fashion based on the extent of kidney injury, as previously described. The scoring system was based primarily on cytoplasmic vacuole formation, tubular cell necrosis, and tubular dilatation. The grading system was as follows: 0 (normal kidney), 1 (1–10% injury, minimal damage), 2 (11-25% injury, mild damage), 3 (26–75% injury, moderate damage), and 4 (76–100% injury, severe damage). The histopathological results were analyzed using a K1-fluo microscope (Nanoscope Systems, Daejeon,

Immunohistochemical (IHC) examination

The sections were initially treated with xylene and ethanol, and then boiled in sodium citrate buffer for 20 min. Next, the sections were treated with 10% H₂O₂ for 10 min to inactivate the endogenous peroxidases. The slides were incubated with antibodies against KIM-1 (1:200), SBP1 (1:400), NGAL (1:2,000), and PKM2 (1:500) at 4 °C for 24 h, followed by incubation with a secondary anti-rabbit antibody (VECTOR, Burlingame, CA, USA) at 24°C for 30 min. HRP-streptavidin reagent (VECTOR Laboratories) was applied at 24°C for 30 min. After staining with 3,3'-diaminobenzidine (DAB; Dako, Agilent, Santa Clara, CA, USA) and hematoxylin (Dako), accompanied by subsequent treatment with ethanol and xylene, the sections were fixed using a mounting solution. The slides were examined under a K1-fluo microscope (Nanoscope Systems, Daejeon, Korea) at 100× magnification. IHC quantification of NGAL, SBP1, KIM-1, and PKM2 was performed using the ImageJ software (Java, USA).

Evaluation of renal oxidative stress

Glutathione (GSH) content enzyme-linked immunosorbent assay (ELISA) kits were purchased from Abcam (Cambridge, UK). One of the predominant markers of free radical-induced oxidative DNA damage, 8-Hydroxy-2'-deoxyguanosine (8-OHdG) has been widely used as a biomarker for oxidative stress [25]. The amount of 8-OHdG in the rat urine samples



was quantified using an ELISA kit (Abcam, Cambridge, UK). All assays were performed in accordance with the manufacturer's instructions.

Analysis of telomere length in the kidney

The average relative telomere length of the genomic DNA was determined from the rat kidney samples using a Relative Rat Telomere Length Quantification Quantitative Polymerase Chain Reaction (qPCR) Assay Kit (ScienCell, San Diego, CA, USA). In this reaction, telomere-specific primers recognize and amplify the telomeric sequences. DNA was extracted using buffers and spin columns based on the instructions for the DNeasy Blood and Tissue Kit (Qiagen, Hilden, Germany). For each DNA sample, two consecutive reactions were performed: one for amplification of a single-copy reference (SCR) gene and the other for amplification of the telomeric sequence. The SCR gene amplifies a 100-bp region on rat chromosome 17 and serves as a reference for calculating the telomere length of the target samples. The PCR reactions were conducted in a final volume of 20 µL, containing the genomic DNA sample (2 ng/ μL), telomere primer, 2× qPCR master mix, and nucleasefree water. Primer-probe Real-Time PCR was performed using a LightCycler 96 Real-Time PCR System (Roche). The PCR conditions were set as follows: denaturation at 95 °C for 10 min, followed by 32 cycles of denaturation at 95 °C for 20 s, annealing at 52 °C for 20 s, and extension at 72 °C for 45 s. All reactions were performed in duplicate. The ratio of telomere repeat copy number (T) to single gene copy number (S) was used to determine relative telomere length (T/S).

Western blot analysis

Protein concentrations were quantified using the bicinchoninic acid (BCA) assay based on the bovine serum albumin (BSA) standard. For denaturation, the proteins were boiled in sample buffer at 96 °C for 5 min. Proteins from tissue (25 µg) and urine (50 µg) were separated on 8-15% gels using sodium dodecyl-sulfate-polyacrylamide gel electrophoresis (SDS-PAGE) and transferred onto polyvinylidene difluoride (PVDF) membranes (Millipore, Billerica, MA, USA). The membranes were blocked in a BSA solution for 1 h at room temperature and incubated with specific primary antibodies overnight at 4 °C. The membranes were washed for 20 min with Tris-buffered saline (TBS) and incubated with HRP-conjugated antirabbit or anti-mouse antibodies (1:20,000) for 1 h at room temperature. The membranes were washed with TBS with Tween (TBS-T) for 30 min. Protein bands were visualized using the LuminoGraph imaging system (ATTO, Tokyo, Japan). Protein expression levels were quantified using the ImageJ software (Java, USA), and band intensities were calculated and presented in a bar graph.

Terminal deoxynucleotidyl transferase dUTP nick end labeling (TUNEL) assay

The kidney sections were dewaxed with xylene, rehydrated with ethanol, and digested with proteinase K for 1 h. The sections were washed with TBS. Apoptosis in rat kidney tissues was identified using a TUNEL test kit (Abcam, Cambridge, UK), following the manufacturer's instructions. The slides were examined using a K1-fluo microscope (Nanoscope Systems, Daejeon, Korea) at 100× magnification.

In vivo tumor xenograft model

Four-week-old male BALB/c nude mice weighing approximately 20 g (Japan SLC Inc., Hamamatsu, Shizuoka, Japan) were housed under controlled temperature and humidity conditions (22 \pm 2 °C) and a 12-h light/dark cycle in laminar flow cabinets with filtered air. Mice were handled aseptically. The experimental protocol was approved by the Institutional Animal Care Committee of the Sungkyunkwan University (SKKUIACUC2023-12-04-1). Mice subcutaneously (s.c.) injected with HCT-116 cells (2×10^7 cells/0.1 mL) in serum-free medium containing 50% Matrigel (BD Biosciences, Franklin Lakes, NJ, USA). The mice were divided into four groups (6 animals per group), as follows: treatment with 0.2 mL DPBS vehicle, CDDP treatment (4 mg/kg, i.p.), CDDP (4 mg/kg, i.p.) + HS1002 (5 mg/kg/d, s.c.), and HS1002 (5 mg/kg/d, s.c.). CDDP was administered once weekly, and HS1002 was administered daily for 18 days. Tumor volume (V) was calculated using the formula: V (mm³) = 0.52 (a × b²), where a is the length and b is the width of the tumor. Body weights were recorded before drug administration and at the end of the experiment. On day 19, mice were euthanized through CO2 asphyxiation.

Statistical analysis

Experiments were conducted in duplicate or triplicate, and all data are presented as the mean \pm standard deviation (S.D.) of at least three independent experiments. Statistical analyses were performed using a one-way analysis of variance (ANOVA) to compare the experimental groups, followed by Tukey's Honestly Significant Difference (HSD) post-hoc test, when appropriate. Statistical significance was set at p < 0.05 and p < 0.01. Statistical analyses were performed using GraphPad Prism Software version 7 (GraphPad Software, San Diego, CA, USA).

Results

Effect of HS1002 on body and organ weight changes in CDDP-treated rats

As shown in Fig. 2A, both the control and HS1002 groups exhibited a normal increase in body weight. However, the CDDP group showed significantly lower body weight than



the control, HS1002, and pretreatment (CDDP + HS1002) groups. In addition, the relative kidney weights significantly increased in the CDDP group but were reduced by HS1002 pretreatment. Kidney weights in both the combination and HS1002 groups were lower than those in the CDDP group (Fig. 2B). These data suggested that HS1002 provides substantial protection against kidney injury in rats.

Protective effect of HS1002 on the biochemical parameters and renal histopathological changes in CDDP-treated rats

Renal function was assessed using serum biochemical analyses. Serum BUN and sCr levels were significantly higher in the CDDP-treated group than in the control group (Fig. 3A). However, HS1002 (10 mg/kg) administration significantly reduced BUN and sCr levels in CDDP-treated rats. Notably, HS1002 restored the impaired renal function caused by CDDP-induced toxicity to varying degrees. Rats treated with HS1002 alone did not show any changes in BUN or sCr levels. These results were consistent with the histopathological changes observed in the kidneys, where HS1002 protected against renal injury following CDDP treatment (Fig. 3B). Microscopic examination of renal tissues in vehicle control rats revealed normal glomerular and renal tubular structures, with no signs of cell necrosis or inflammatory infiltration. In contrast, CDDP-treated rats exhibited significant renal tissue damage, including vacuolization of the renal cortex, necrosis, and inflammatory infiltration. However, the number of infiltrating inflammatory cells decreased in the HS1002-pretreated group. In HS1002pretreated group, the kidney injury score was significantly lower compared with the CDDP group (Fig. 3C), suggesting that HS1002 may offer protection against CDDP-induced nephrotoxicity.

Effects of HS1002 on the urinary excretion of kidney injury biomarkers in CDDP-treated rats

To assess whether HS1002 protects against kidney injury, the levels of KIM-1, NGAL, and SBP1 in urine and kidney tissues were measured using Western blot analysis. As shown in Fig. 4A and 4B, CDDP treatment significantly increased the urinary excretion and expression of NGAL, KIM-1, and SBP1 compared to that in the control group. However, HS1002 (10 mg/kg) administration significantly reduced the levels of these biomarkers in CDDP-exposed rats. IHC staining revealed significant expression of KIM-1, NGAL, SBP1, and PKM2 in injured proximal tubules of the kidneys. Similarly, these biomarkers were highly expressed in the kidneys of the CDDP-treated animals. However, HS1002 administration markedly reduced the expression of these biomarkers in the renal tissues of the treated rats (Fig. 4C and 4D).

Protective effects of HS1002 on apoptosis in the kidney of CDDP-treated rats

To confirm the extent of apoptosis in the kidney tissues of the CDDP-treated rats, the expression of apoptosis-related proteins was quantified (Fig. 5A and 5B). CDDP notably reduced the protein expression of Bcl-2 and increased p53 and Bax expression. However, HS1002 administration reversed these effects, restoring the expression of apoptosis-related proteins in the kidneys of CDDP-treated rats. As shown in Fig. 5C and 5D, the TUNEL assay revealed a higher number of TUNEL-positive cells in the CDDP group compared with the control group, particularly in the renal cortex. HS1002 treatment alone did not significantly alter the number of TUNEL-positive cells. However, HS1002 pretreatment before CDDP administration resulted in a marked decrease in the number of TUNEL-positive cells. Interestingly, TUNELstained cells were primarily scattered throughout the kidney tubules after CDDP injection. These results indicate that HS1002 effectively protected against apoptosis in the kidneys of CDDP-treated rats.

Protective effects of HS1002 against oxidative damage in the kidneys of CDDP-treated rats

Oxidative stress injury is one of the most important mechanisms underlying CDDP-induced renal toxicity in rats. GSH levels in rats treated with CDDP are summarized in Fig. 6A. To validate the relationship between oxidative stress and renal toxicity *in vivo*, 8-OHdG levels were measured in rat urine samples. As shown in Fig. 6B, the 8-OHdG concentration markedly increased in rat urine after CDDP administration. Moreover, the CDDP-induced increases in renal 8-OHdG and malondialdehyde (MDA) levels were attenuated by HS1002 (10 mg/kg).

Inhibitory effect of HS1002 on telomere length in CDDP-treated rats

Telomere length ratio, often represented as the telomere-to-single-copy gene (T/S) ratio, is emerging as a potential biomarker for nephrotoxicity, particularly in studies involving chronic kidney disease (CKD). In the context of nephrotoxicity, shortened telomeres in kidney cells can indicate cellular aging, oxidative stress, and damage, which are characteristic of toxic injury to the kidneys. As shown in Fig. 6C, telomere length ratio was significantly decreased in kidney tissue after CDDP injection compared to controls. However, HS1002 pretreatment slightly elevated the telomere length ratio in renal tissues of rats.

HS1002 regulated ERK/MAPK signaling pathway in the kidneys of CDDP-treated rats

To investigate the protective mechanism of HS1002 against CDDP-induced AKI, the pro-survival PI3K/Akt signaling pathway was examined using western blot

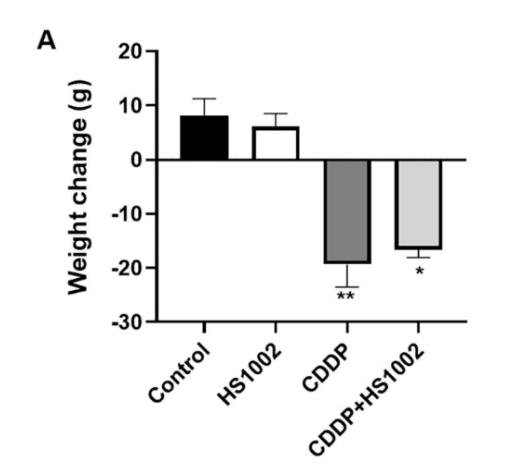


analysis. The results demonstrated that CDDP significantly activated Akt and AMP-activated protein kinase (AMPK) in the kidneys of rats compared to the controls, in addition to a concomitant reduction in phosphatase and tensin homolog (PTEN) expression (Fig. 7). However, HS1002 pretreatment suppressed Akt and AMPK phosphorylation and simultaneously restored PTEN expression in rat kidneys. These findings suggest that HS1002 modulates apoptosis, at least in part, by acting on the Akt signaling pathway. The levels of phosphorylated p38, ERK1/2, and JNK were

markedly higher in the CDDP group than in the control group. In contrast, the expression of these proteins was significantly reduced in the group pretreated with HS1002 (Fig. 8).

Renoprotective effects of HS1002 in the CDDP-induced tumor xenograft model

To evaluate the anticancer effects of CDDP in a xenograft tumor model, nude mice were inoculated with HCT-116 cells and treated with CDDP (4 mg/kg, i.p., once weekly) or HS1002 (5 mg/kg, s.c., daily) for 18 days. Animals in the CDDP-treated group exhibited a significant decrease in



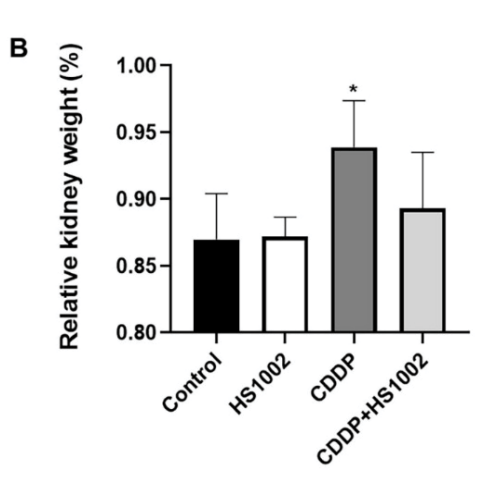


Figure 2: Effects of nephrotoxicity on body and kidney weight changes in rats. (A) Body weight change in cisplatin (CDDP)-treated rats. (B) Relative kidney weight in CDDP-treated rats. Data are expressed as the mean \pm S.D from three repeated experiments. Statistical analyses were performed using a one-way analysis of variance (ANOVA) to compare the experimental groups, followed by Tukey's post-hoc test, *p < 0.05 and **p < 0.01 compared to control group, relative kidney weight (%) = [kidney weight/body weight] \times 100.

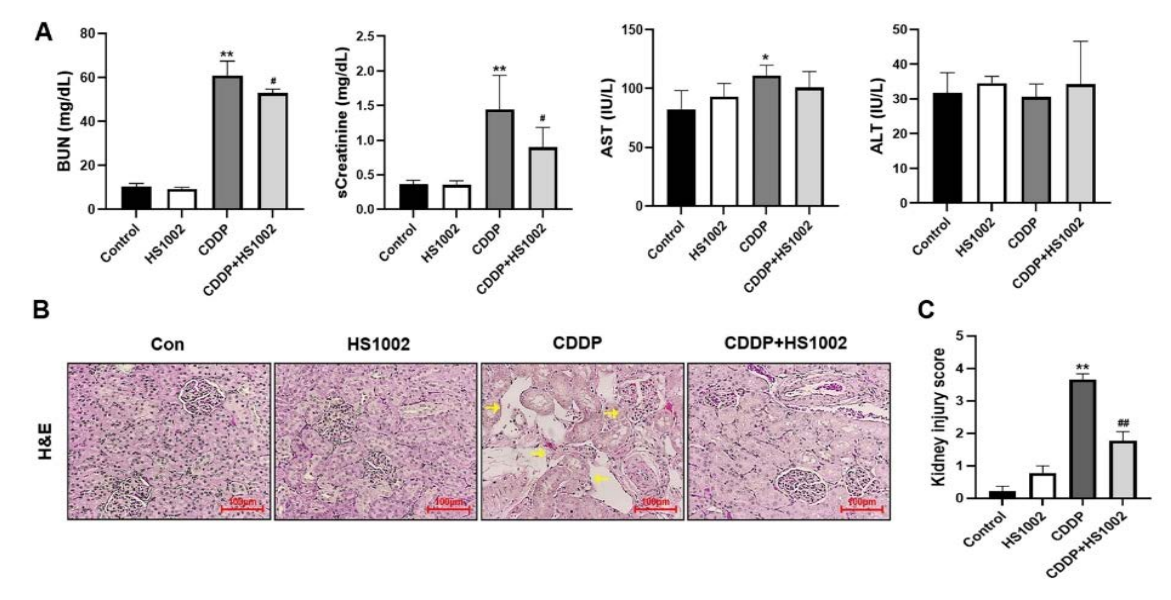


Figure 3: Effects of HS1002 on cisplatin (CDDP)-induced nephrotoxicity in rats. (A) Serum biochemical parameters (blood urea nitrogen [BUN], creatinine [sCr], aspartate transaminase [AST], and alanine transaminase [ALT]) were measured to assess kidney damage in rats. (B) Hematoxylin-eosin (H&E) staining of representative kidney tissues in rats. Yellow arrows indicate infiltration and tissue necrosis in the proximal tubules. (C) Histopathological injury score. Data are expressed as the mean \pm S.D from three repeated experiments. Statistical analyses were performed using a one-way analysis of variance (ANOVA) to compare the experimental groups, followed by Tukey's post-hoc test, $^*p < 0.05$ and $^{**}p < 0.01$ compared to the control group, $^*p < 0.05$ and $^{**}p < 0.01$ compared to the CDDP-treated group.



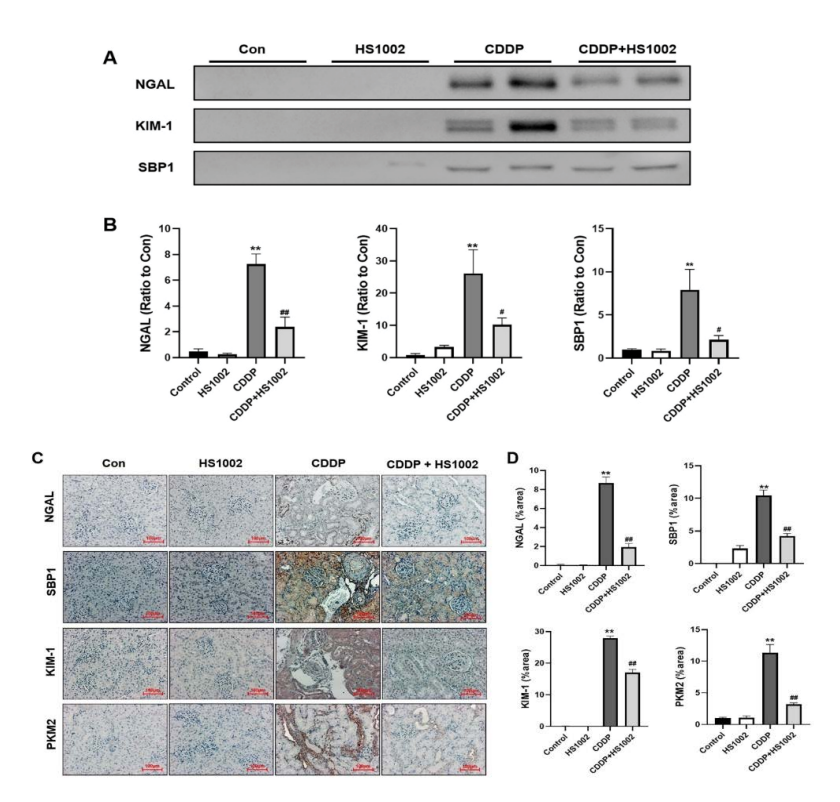


Figure 4: Kidney injury biomarkers in the urine and kidneys after cisplatin (CDDP) administration in rats. (A) Western blot analysis of nephrotoxicity biomarkers in rat urine. (B) Quantification of NGAL, KIM-1, and SBP1 expressions. (C) Immunohistochemical (IHC) staining expression levels of nephrotoxicity biomarkers in rat kidneys. (D) The percentage of nephrotoxicity biomarkers in the positive area was calculated. Data are expressed as the mean \pm S.D from three repeated experiments. Statistical analyses were performed using a one-way analysis of variance (ANOVA) to compare the experimental groups, followed by Tukey's post-hoc test. **p < 0.01 compared to the control group; *p < 0.05 and **p < 0.01 compared to the CDDP-treated group.

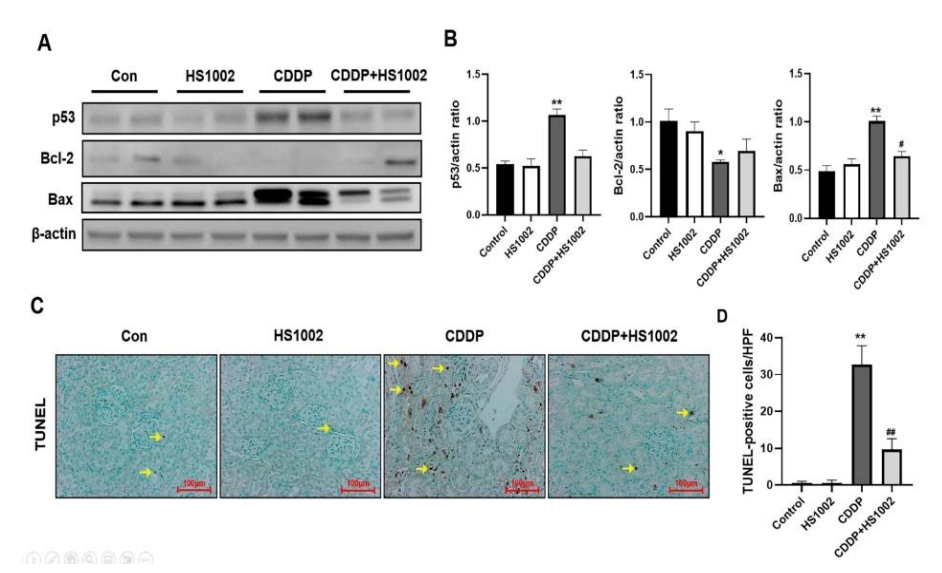


Figure 5: Effect of HS1002 on apoptosis in the kidneys of cisplatin (CDDP)-treated rats. (A) Western blot analysis of p53, Bcl-2, and Bax in representative rat kidney tissues. (B) Quantification of p53, Bcl-2, and Bax expression all normalized to β-actin ratio used as the loading control. (C) Detection of apoptosis in kidney tissues of rats using the TUNEL assay. Yellow arrows indicate apoptotic cells population in the kidney tissues. (D) Quantification of TUNEL-positive cells was performed using ImageJ software. Data are expressed as the mean \pm S.D from three repeated experiments. Statistical analyses were performed using a one-way analysis of variance (ANOVA) to compare the experimental groups, followed by Tukey's post-hoc test. *p < 0.05 and **p < 0.0



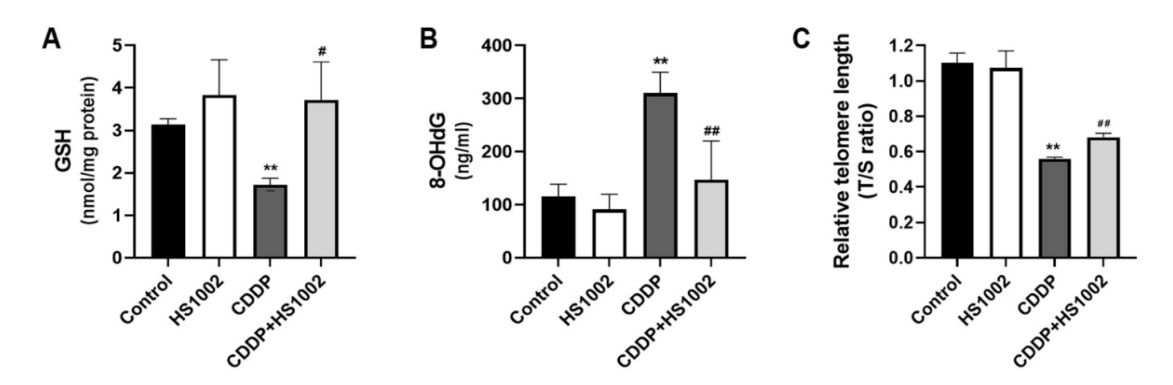


Figure 6: Effects of HS1002 on oxidative damage in the kidneys of CDDP-treated rats. (A) The glutathione (GSH) level was measured in the kidneys of rats. (B) The 8-OHdG level as measured in the urine of rats to assess DNA damage. (C) Average relative telomere length shown as T/S ratios of CDDP-treated rats using quantitative polymerase chain reaction (qPCR). Data are expressed as the mean \pm S.D from three repeated experiments. Statistical analyses were performed using a one-way analysis of variance (ANOVA) to compare the experimental groups, followed by Tukey's post-hoc test. **p < 0.01 compared to the control group, *p < 0.05 and **p < 0.01 compared to the CDDP-treated group.

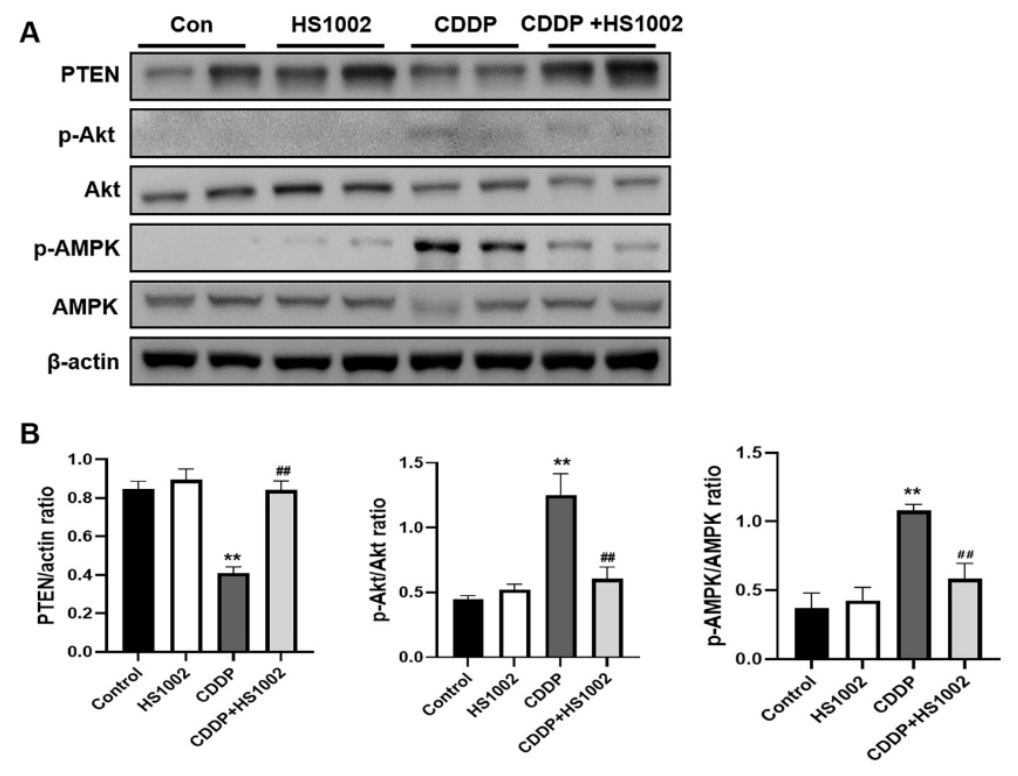


Figure 7: HS1002 regulates the PI3K/Akt signaling pathway in CDDP-treated rats. (A) PTEN, p-Akt, Akt, p-AMPK, and AMPK levels in the kidneys of rats treated with CDDP followed by HS1002 were quantified using Western blot analysis. (B) Quantitative analysis of PTEN, p-Akt, and p-AMPK expression all normalized to β -actin ratio used as the loading control. Data are expressed as the mean \pm S.D from three repeated experiments. Statistical analyses were performed using a one-way analysis of variance (ANOVA) to compare the experimental groups, followed by Tukey's post-hoc test. **p < 0.01 compared to the control group, **p < 0.01 compared to the CDDP-treated group.

body weight (Fig. 9A). In the CDDP-treated groups, tumor volumes and weights were significantly reduced compared to those in the control group (Fig. 9B and 9C). HS1002 administration with CDDP dramatically suppressed tumor growth in a manner similar to that observed in the CDDP-treated animals. IHC staining revealed that the antitumor

activity of the combination treatment with CDDP and HS1002 was associated with reduced Ki-67 expression in tumor tissues (Fig. 9D and 9E). These results suggest that combination treatment with HS1002 and CDDP enhances the CDDP-mediated anticancer activity. Therefore, HS1002 did not interfere with the anticancer efficacy of CDDP in the



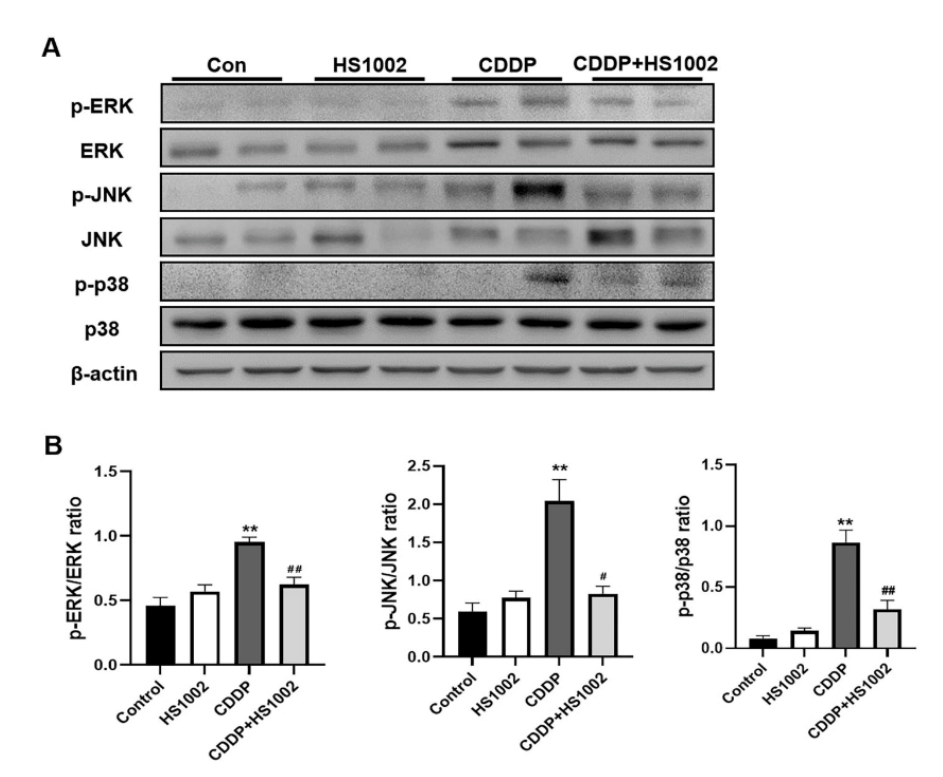


Figure 8: HS1002 regulates the ERK/MAPK signaling pathway in CDDP-treated rats. (A) p-ERK, ERK, p-JNK, JNK, p-p38, and p38 levels in the kidneys of rats were quantified using Western blot analysis. (B) Quantitative analysis of p-ERK, ERK, p-JNK, JNK, p-p38, and p38 expression all normalized to β -actin ratio used as the loading control. Data are presented as mean \pm S.D. from three repeated experiments. Statistical analyses were performed using a one-way analysis of variance (ANOVA) to compare the experimental groups, followed by Tukey's post-hoc test. **p < 0.01 compared to the control group; *p < 0.05 and **p < 0.01, compared to the CDDP-treated group.

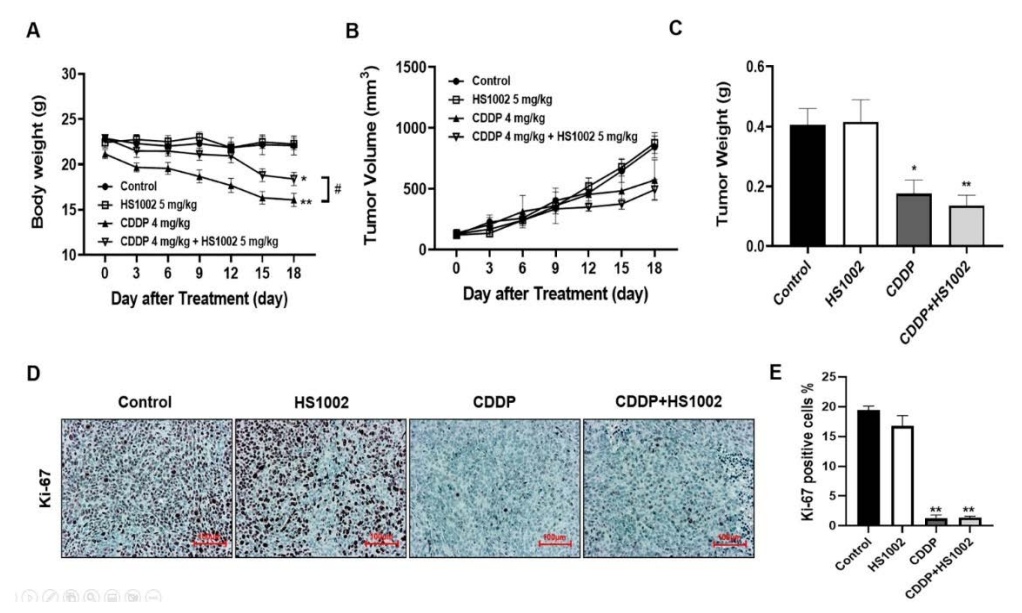


Figure 9: Protective effect of HS1002 on CDDP-induced nephrotoxicity in tumor xenograft mice inoculated with HCT-116 cells. (A) Effect of HS1002 on body weight changes in tumor xenograft mice treated with CDDP. (B) Each graph shows the mean tumor volumes in tumor xenograft mice after drug treatment for 18 days. (C) Each bar represents the mean tumor weight. Values are the mean \pm S.D. of six mice per group. Statistical analyses were performed using one-way ANOVA followed by Tukey's HSD post hoc test for multiple comparisons. Data are presented as mean \pm S.D. *p < 0.05 and **p < 0.01 compared to the control group; *p < 0.05 compared to the CDDP-treated group. (D) Representative IHC expression of Ki-67 in the experimental groups of the tumor xenograft mouse model. Images are representative of three animals per experimental group (magnification, × 100; scale bar = 100 μ m). (E) Densitometric analysis showed the expression of Ki-67 in the kidney of mice. **p < 0.01 compared to the control group.



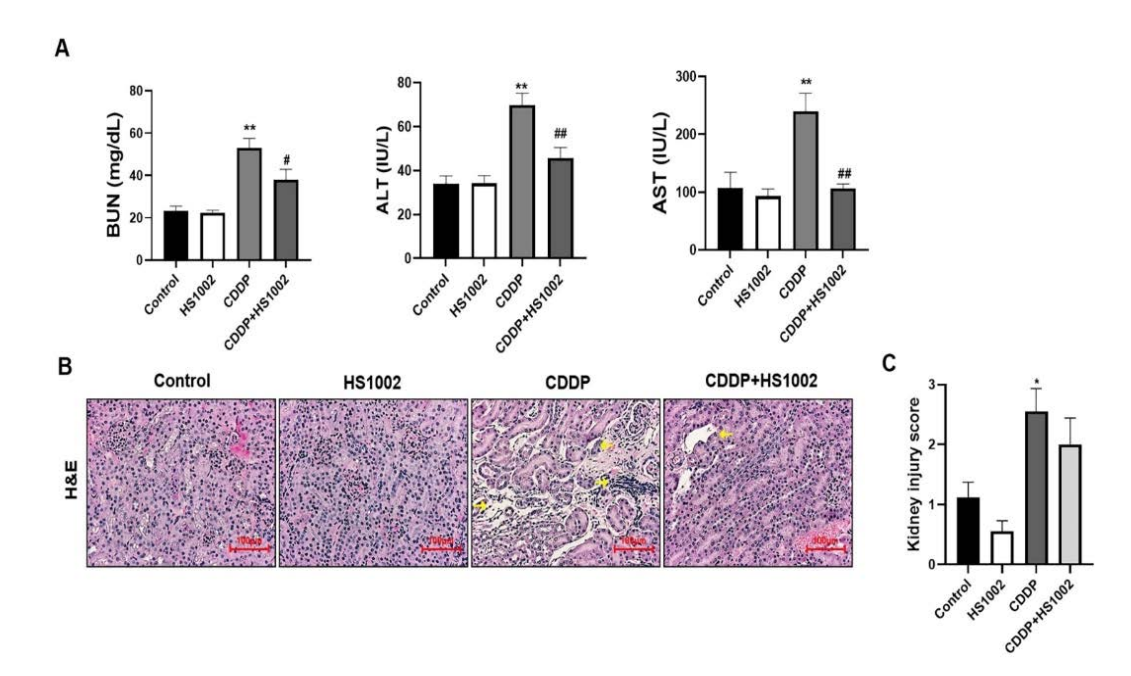


Figure 10: Protective effect of HS1002 on CDDP-induced nephrotoxicity in tumor xenograft mice inoculated with HCT-116 cells. (A) Serum biochemical parameters were measured in mice. Values are the mean \pm SD of six rats per group. Statistical analyses were performed using one-way ANOVA followed by Tukey's HSD post hoc test for multiple comparisons. **p < 0.01 compared to the control group; $^{\#}p < 0.05$; $^{\#\#}p < 0.01$ compared to the CDDP-treated group. (B) Representative histology of H&E-stained kidney sections in the experimental groups of a tumor xenograft mouse model. The cortex from CDDP-treated mice exhibited a normal-sized renal cortex and a lower incidence of tubular and medulla injury (stars) and displayed a normal histological structure of thin tubules and collecting ducts. Images are representative of three animals per experimental group (magnification ×100, bar = 100 µm). (C) Effect of HS1002 on kidney injury score in rat kidneys. Values are the mean \pm S.D. of six mice per group. Statistical analyses were performed using one-way ANOVA followed by Tukey's HSD post hoc test for multiple comparisons. *p < 0.05 compared to the control group.

xenograft tumor model. Serum BUN was also significantly elevated in the CDDP-treated group compared to those in the control group, indicating severe kidney damage in tumorbearing mice treated with CDDP. HS1002 administration significantly reduced BUN levels in the CDDP-treated mice, with no changes observed in BUN levels following HS1002 treatment alone. ALT and AST levels were also significantly increased in the CDDP group and decreased following HS1002 co-administration (Fig. 10A). As shown in Fig. 10B and 10C, HS1002 protected against CDDP-induced proximal tubular damage and renal architectural disruption.

To assess the expression of NGAL and PKM2 in the kidney tissues of CDDP-treated tumor-bearing mice, protein levels were measured using western blot analysis. As shown in Fig. 11A and 11B, CDDP (4 mg/kg) treatment significantly increased the expression of NGAL and PKM2 compared to the controls. However, administration of HS1002 markedly reduced the levels of NGAL and PKM2 in CDDP-treated tumor-bearing mice. The expression of these biomarkers was further examined using IHC staining (Fig. 11C and 11D). NGAL and PKM2 were primarily expressed in the damaged proximal tubules of the kidneys.

Discussion

CDDP induces significant toxicities, including neurotoxicity, ototoxicity, and nephrotoxicity, which limit its permissible dosage range. Reducing these side effects is crucial to improve the efficacy of chemotherapy in patients with cancer. Recently, various preventive strategies to mitigate the side effects of CDDP, while preserving its chemotherapeutic effectiveness, have been investigated. Among these strategies, it has been reported that GV1001, derived from the hTERT peptide, and GnRH agonists can reduce nephrotoxicity [23,24]. Therefore, HS1002, derived from both the hTERT peptide and GnRH, was hypothesized to have a nephroprotective effect. The present study aimed to evaluate the protective effects of HS1002 in the CDDPinduced AKI model, a well-established model for assessing the nephroprotective efficacy of pharmaceuticals in various rodent AKI models [7,26,27].

A single administration of CDDP at the therapeutically used dose of 6 mg/kg has been shown to induce nephrotoxicity in rats. This study found that CDDP caused AKI and tubular cell apoptosis in renal tissues. In addition to the decline in renal function caused by CDDP, there was a significant increase in the sCr and BUN levels. A notable elevation

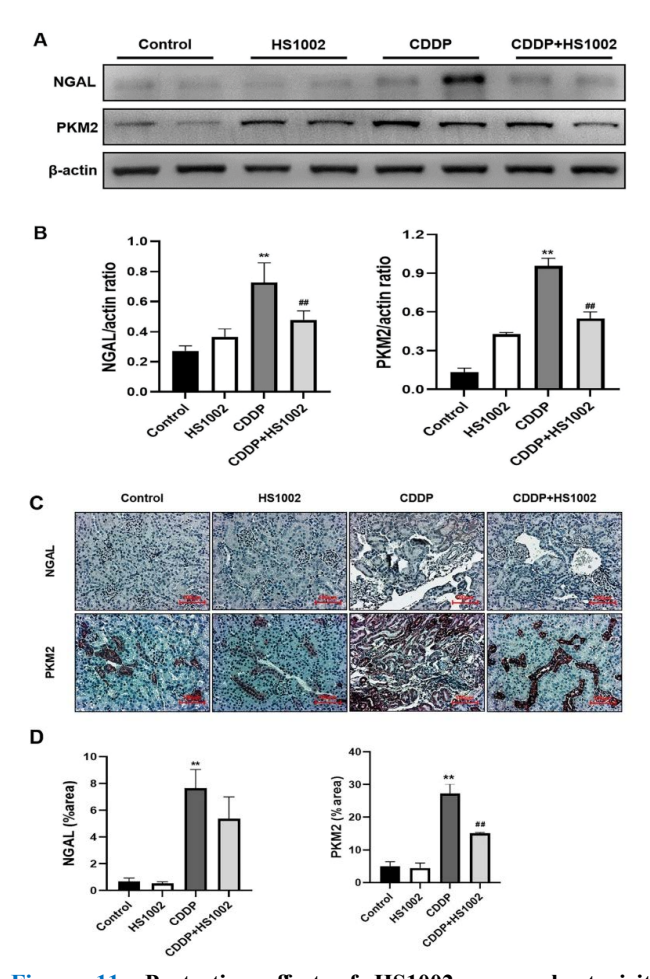


Figure 11: Protective effect of HS1002 on nephrotoxicity biomarkers in CDDP-induced nephrotoxicity in tumor xenograft mice inoculated with HCT-116 cells. (A) Nephrotoxicity biomarkers were measured in the kidney of mice. Representative Western blots of NGAL and PKM2 from triplicate experiments are shown. (B) Densitometric analysis showed the expression of NGAL and PKM2 in the kidney of mice. **p < 0.01 compared to the control group; $^{\#}p < 0.01$ compared to the CDDP-treated group. (C) Representative immunohistochemical staining of NGAL and PKM2 in the kidney of mice with CDDP-induced nephrotoxicity. Original magnification ×100, scale bar: 50 μm. (**D**) Densitometric analysis showed the expression of NGAL and PKM2 in the kidney of mice. **p < 0.01 compared to the control group; **p < 0.01 compared to the CDDP-treated group.

in the urinary excretion of novel AKI biomarkers such as KIM-1, NGAL, and SBP1 was also observed in CDDPtreated rats. However, the present study showed that HS1002 administration substantially reduced the occurrence of CDDPinduced AKI. HS1002 administration led to improvements in sCr, BUN, and biomarker levels, indicating that HS1002 has the potential to restore kidney function impaired by CDDP. Furthermore, the kidney tissues in the CDDP-treated groups exhibited normal histopathology following HS1002 pretreatment. Several mechanisms including inflammation, oxidative stress, DNA damage, and apoptosis have been identified as key contributors to the development of CDDPinduced nephrotoxicity [28,29].

Scientific evidence has indicated a strong correlation between the formation of ROS in the renal proximal tubules and the development of CDDP-induced nephrotoxicity [30,31]. Oxidative stress occurs when there is an imbalance between the antioxidant and oxidant systems, thereby leading to cellular degradation. Oxidative stress and the resulting production of ROS play crucial roles in maintaining kidney function and structure under both physiological and pathological conditions [32]. This stress often impairs the structural components of cells such as lipids, proteins, and mitochondria [32]. In the present study, 8-OHdG was selected as a marker of oxidative stress caused by CDDP and measured in CDDP-induced AKI. CDDP injection significantly increased 8-OHdG levels in the rat urine, whereas HS1002 pretreatment effectively reduced 8-OHdG levels, thereby preventing DNA damage.

In the previous study, GV1001, which is derived from the hTERT peptide, has shown protective properties against renal injury [23]. Similarly, the present study showed that administration of HS1002 significantly reduced oxidative stress in the renal tissues of CDDP-treated rats. However, the relationship between telomere shortening and kidney injury remains unclear. Notably, oxidative stress has been identified as a significant factor contributing to changes in telomere length. Telomeres are tandemly repeating DNA sequences (5'-TTAGGG-3') located at the ends of chromosomes that protect genetic information and prevent DNA degradation [33]. Telomeres naturally shorten with aging, a process influenced by environmental factors and genetic alterations [34].

In the present study, telomere shortening has also been observed following CDDP exposure, suggesting that oxidative stress contributes to telomere dynamics during kidney injury. The kidneys of CDDP-treated rats exhibited increased levels of oxidative stress, which correlated with a significant increase in apoptosis. To validate the occurrence of CDDP-induced apoptosis, apoptotic cells were quantified using a TUNEL assay. The number of TUNEL-positive cells increased significantly in kidney sections of CDDP-treated rats. However, HS1002 treatment demonstrated a protective effect against apoptosis in kidneys affected by CDDP-induced AKI. The present findings provide further evidence that CDDP administration leads to oxidative damage in kidneys, as indicated by an increase in the number of TUNEL-positive cells. HS1002 administration strongly inhibited apoptosis, reduced kidney injury marker levels, and mitigated renal histological alterations in rats with CDDP-induced AKI. These results highlight the significant reduction in CDDPinduced apoptosis in kidney tissues following HS1002 treatment, thus suggesting its potential as a novel therapeutic approach for treating CDDP-induced AKI.



Biological activities, such as transcriptional regulation and cell survival, are governed by the PI3K/Akt pathway [35]. Activation of the PI3K/Akt pathway in renal tubular cells has been demonstrated following CDDP treatment [36,37]. CDDP may also stimulate the expression of DNA repair genes, including excision repair cross complementation 1 and thymidine phosphorylase, by activating the PI3K/Akt, ERK, and p38 signaling pathways [38]. An increase in renal tubular epithelial cell apoptosis has been reported in PI3K knockout mice, suggesting that the PI3K/Akt pathway plays an important role in maintaining renal function during CDDP-induced kidney injury [39]. Similarly, when PI3K was inhibited by wortmannin or LY294002 in a previous study, reduction of CDDP-induced Akt and elevation of caspase-3 and caspase-9 activation (dependent on mitochondrial pathways) was observed, accelerating the process of cellular death [40]. The present study showed that CDDP activates Akt, promoting cell survival signaling. The increase in Akt expression was accompanied by the inhibition of PTEN, a protein that negatively regulates the intracellular concentrations of phosphatidylinositol-3,4,5-trisphosphate, thereby leading to the down-regulation of the PI3K/Akt pathway [41]. HS1002 administration restored PTEN levels and subsequently reduced Akt phosphorylation, indicating a potential decrease in the activation of this pro-survival protein. CDDP activates ERK, JNK, and p38 both in vitro and in vivo in a dose- and time-dependent manner [15]. Although ERK1/2 is typically considered as a pro-survival factor, it may also play a role in the pro-apoptotic response to DNA damage by activating p53 transcription and promoting BAX expression [42]. ERK1/2 is essential for CDDP-induced renal tubular cell apoptosis [43], which can be inhibited by blocking ERK activation [44]. In rat kidneys, phospho-ERK1/2 activation by CDDP occurs alongside the upregulation of p53 and BAX expression, suggesting a potential link between ERK1/2 activation and apoptotic cell death. HS1002 administration reduced the production of pro-apoptotic proteins, accompanied by the inhibition of ERK1/2 activation.

Conclusion

In summary, the results of the present study indicate that the administration of HS1002 has a beneficial effect on CDDP-induced AKI by inhibiting the ERK1/2 and PI3K/Akt signaling pathways. This effect is consistent with the antiapoptotic and antioxidant properties of HS1002. This study demonstrates that HS1002 exerts a protective effect against CDDP-induced AKI by inhibiting oxidative stress, telomere shortening, and apoptosis. In addition, HS1002 did not exhibit any adverse effects on renal tubular cells. However, the mechanism of action of GnRH agonists and their potential impact on individual hormone levels remain unclear. Additional studies are required to determine whether HS1002 can reduce CDDP nephrotoxicity without compromising

the chemotherapeutic efficacy in xenograft mouse models. Collectively, these findings suggest that HS1002 has the potential to be an effective preventive therapy to alleviate the occurrence of AKI in patients undergoing CDDP chemotherapy.

Author's Contributions

JHH and HSK conceptualized and designed the experiments. JHH, HJN, JRK, and HL carried out the experiments. JHH and HJN analyzed the experimental data. HL and JHP made substantial contributions to the interpretation of data and supervised the present study. JHH, JHP, and HSK wrote, reviewed, and revised the manuscript. All authors have read and approved the final manuscript. JHH, HJN, JRK, HL, JHP, and HSK confirm the authenticity of all the raw data

Acknowledgements: Not applicable.

Declaration of Competing Interest

The authors declare no conflict of interest.

Availability of data and materials

The data that support the findings of this study are available from the corresponding author upon reasonable request.

Consent for Publication

The author approves the publication of this manuscript.

Ethics approval and consent to participate

All applicable international, national, and institutional guidelines for animal care and use were adhered to. All animal procedures were performed in accordance with the ethical standards of the institution where the studies were conducted. Consent to participate is not applicable, as no human subjects were involved.

Funding

This work was supported by a grant from the National Research Foundation (NRF) of Korea (grant number: NRF-2022R1A4A1018930).

References

- Miller R, Tadagavadi R, Ramesh G, et al. Mechanisms of cisplatin nephrotoxicity. Toxins (Basel) 2 (2010): 2490-2518.
- Dasari S, Tchounwou P. Cisplatin in cancer therapy: Molecular mechanisms of action. Eur J Pharmacol 740 (2014): 364–378.
- 3. Oun R, Moussa Y, Wheate N. The side effects of platinum-



- based chemotherapy drugs: A review for chemists. Dalton Transact 47 (2018): 6645–6653.
- 4. Tang C, Livingston M, Safirstein R, et al. Cisplatin nephrotoxicity: New insights and therapeutic implications. Nat Rev Nephrol 19 (2023): 53–72.
- 5. Shin Y, Kim K, Park Y, et al. Discovery of urinary metabolomic biomarkers for early detection of acute kidney injury. Mol Biosyst 12 (2016): 133–144.
- 6. Kim K, Yang H, Song H, et al. Identification of a sensitive urinary biomarker, selenium-binding protein 1, for early detection of acute kidney injury. J Toxicol Environ Health 80 (2017): 453–464.
- 7. Kim J, Yadav D, Kim S, et al. Anti-cancer effect of GV1001 for prostate cancer: Function as a ligand of GnRH. Endocr Relat Cancer 26 (2019): 147–162.
- 8. Won A, Kim J, Choi S, et al. Discovery of urinary metabolomic biomarkers for early detection of acute kidney injury. Mol Biosyst 12 (2016): 133–144.
- Siddik Z. Cisplatin: Mode of cytotoxic action and molecular basis of resistance. Oncogene 22 (2003): 7265– 7279.
- 10. Izzedine H, Perazella M. Anticancer drug-induced acute kidney injury. Kidney Int Rep 2 (2017): 504–514.
- 11. Chirino Y, Pedraza-Chaverri J. Role of oxidative and nitrosative stress in cisplatin-induced nephrotoxicity. Exp Toxicol Pathol 61 (2009): 223–242.
- 12. Atessahin A, Yilmaz S, Karahan I, et al. Effects of lycopene against cisplatin-induced nephrotoxicity and oxidative stress in rats. Toxicology 212 (2005): 116–123.
- 13. Mitazaki S, Hashimoto M, Matsuhasi Y, et al. Interleukin-6 modulates oxidative stress produced during the development of cisplatin nephrotoxicity. Life Sci 92 (2013): 694–700.
- 14. Brozovic A, Ambriović-Ristov A, Osmak M. The relationship between cisplatin-induced reactive oxygen species, glutathione, and BCL-2 and resistance to cisplatin. Crit Rev Toxicol 40 (2010): 347–359.
- Pabla N, Dong Z. Cisplatin nephrotoxicity: Mechanisms and renoprotective strategies. Kidney Int 73 (2008): 994– 1007.
- 16. Huang Y, Tsai M, Hsieh P. Galangin ameliorates cisplatininduced nephrotoxicity by attenuating oxidative stress, inflammation, and cell death in mice through inhibition of ERK and NF-kappaB signaling. Toxicol Appl Pharmacol 329 (2017): 128–139.
- 17. Craik D, Fairlie D, Liras S, et al. The future of peptide-

- based drugs. Chem Biol Drug Des 81 (2013): 136–147.
- 18. Sharma K, Sharma K, Sharma A, et al. Peptide-based drug discovery: Current status and recent advances. Drug Discov Today 28 (2023): 103464.
- 19. Wang L, Wang N, Zhang W, et al. Therapeutic peptides: Current applications and future directions. Signal Transduct Target Ther 7 (2022): 48.
- 20. Muttenthaler M, King G, Adams D, et al. Trends in peptide drug discovery. Nat Rev Drug Discov 20 (2021): 309–325.
- 21. Liu F, Luo E, Flora D, et al. A synthetic route to human insulin using isoacyl peptides. Angew Chem 126 (2014): 4064–4068.
- 22. Groß A, Hashimoto C, Sticht H, et al. Synthetic peptides as protein mimics. Front Bioeng Biotechnol 3 (2016): 211.
- 23. Koo T, Yan J, Yang J. Protective effect of peptide GV1001 against renal ischemia-reperfusion injury in mice. Transplant Proc 46 (2014): 1117–1122.
- 24. Nomura K, Ando T, Demura H. Leuprolide acetate prevents toxic effects of cisplatin on the kidneys and gastrointestinal tract. Endocr J 42 (1995): 315–321.
- 25. Valavanidis A, Vlachogianni T, Fiotakis C, et al. 8-hydroxy-2' -deoxyguanosine (8-OHdG): A critical biomarker of oxidative stress and carcinogenesis. J Environ Sci Health C 27 (2009): 120–139.
- 26. Park Y, Kim K, Park J, et al. Protective effects of dendropanoxide isolated from Dendropanax morbifera against cisplatin-induced acute kidney injury via the AMPK/mTOR signaling pathway. Food Chem Toxicol 145 (2020): 111605.
- 27. Xu Y, Ma H, Shao J et al. A role for tubular necroptosis in cisplatin-induced AKI. J Am Soc Nephrol 26 (2015): 2647–2658.
- 28. Volarevic V, Djokovic B, Jankovic M, et al. Molecular mechanisms of cisplatin-induced nephrotoxicity: A balance on the knife edge between renoprotection and tumor toxicity. J Biomed Sci 26 (2019): 25.
- 29. Herrera-Pérez Z, Gretz N, Dweep H. A comprehensive review on the genetic regulation of cisplatin-induced nephrotoxicity. Curr Genomics 17 (2016): 279–293.
- 30. McSweeney K, Gadanec L, Qaradakhi T, et al. Mechanisms of cisplatin-induced acute kidney injury: Pathological mechanisms, pharmacological interventions, and genetic mitigations. Cancers (Basel) 13 (2021): 1572.
- 31. Ozbek E. Induction of oxidative stress in kidney. Int J Nephrol 2012 (2012): 465897.



- 32. Ahmed W, Lingner J. Impact of oxidative stress on telomere biology. Differentiation 99 (2018): 21–32.
- 33. Fernandes S, Dsouza R, Khattar E. External environmental agents influence telomere length and telomerase activity. Environ Toxicol Pharmacol 85 (2021): 103633.
- 34. Song G, Ouyang G, Bao S: The activation of Akt/PKB signaling pathway and cell survival. J Cell Mol Med 9 (2005): 59–71.-
- 35. Ju S, Kang J, Bae J, et al. The flavonoid apigenin ameliorates cisplatin-induced nephrotoxicity through reduction of p53 activation and promotion of PI3K/Akt pathway. Evid Based Complement Alternat Med 2015 (2015): 186436.
- 36. Li Y, Li X, Zheng W, et al. Functionalized selenium nanoparticles with nephroprotective activity: The important roles of ROS-mediated signaling pathways. J Mater Chem B 1 (2013): 6365–6372.
- 37. Liu C, Lim Y, Hu M, et al. Fucoxanthin enhances cisplatininduced cytotoxicity via NFκB-mediated pathway and downregulates DNA repair gene expression in human hepatoma HepG2 cells. Mar Drugs 11 (2013): 50–66.
- 38. Kuwana H, Terada Y, Kobayashi T, et al. The phosphoinositide-3 kinase γ -Akt pathway mediates renal

- tubular injury in cisplatin nephrotoxicity. Kidney Int 73 (2008): 430–445.
- 39. Kaushal G, Kaushal V, Hong X et al. Role and regulation of activation of caspases in cisplatin-induced injury to renal tubular epithelial cells. Kidney Int 60 (2001): 1726–1736.
- 40. Song M, Salmena L, Pandolfi P. The functions and regulation of the PTEN tumour suppressor. Nat Rev Mol Cell Biol 13 (2012): 283–296.
- 41. Cagnol S, Chambard J. ERK and cell death: Mechanisms of ERK-induced cell death—Apoptosis, autophagy and senescence. FEBS J 277 (2010): 2–21.
- 42. Gao S, Chen T, Choi M, et al. Cyanidin reverses cisplatininduced apoptosis in HK-2 proximal tubular cells through inhibition of ROS-mediated DNA damage and modulation of the ERK and AKT pathways. Cancer Lett 333 (2013): 36–46.
- 43. Potočnjak I, Škoda M, Pernjak-Pugel E, et al. Oral administration of oleuropein attenuates cisplatin-induced acute renal injury in mice through inhibition of ERK signaling. Mol Nutr Food Res 60 (2016): 530–541.
- 44. Wang Y, Tang C, Wang S, et al. Crosstalk between oxidative stress and inflammation in cisplatin-induced nephrotoxicity. Int J Mol Sci 20 (2019): 4728.



This article is an open access article distributed under the terms and conditions of the Creative Commons Attribution (CC-BY) license 4.0